Supplementary Information (SI) for Journal of Materials Chemistry C.

Supporting Information

Photo-driven All-2D van der Waals metal-semiconductor field-effect transistors for high-performance photodetection

Chunyu Li[a], Zhiming Wu[a,b,*], Meiyu He[a], Chaoyi Zhang[a], Silu Peng[a], Jiayue Han[a], Laijiang Wei[a] Xiang Dong[a,b], Jun Gou[a,b,*] , Jun Wang[a,b,c,*] and Yadong Jiang[a,b]

a School of Optoelectronic Science and Engineering, University of Electronic Science and Technology of China, Chengdu, 610054, China.

b State Key Laboratory of Electronic Thin Films and Integrated Devices, University of Electronic Science and Technology of China, Chengdu 610054, China.

c Key Laboratory of Science and Technology on Infrared Detector, Luoyang 471099, China

*Correspondence should be addressed to Z. Wu (Email: zmwu@uestc.edu.cn); J. Wang (Email: wjun@uestc.edu.cn); J. Gou (Email: goujun@uestc.edu.cn).

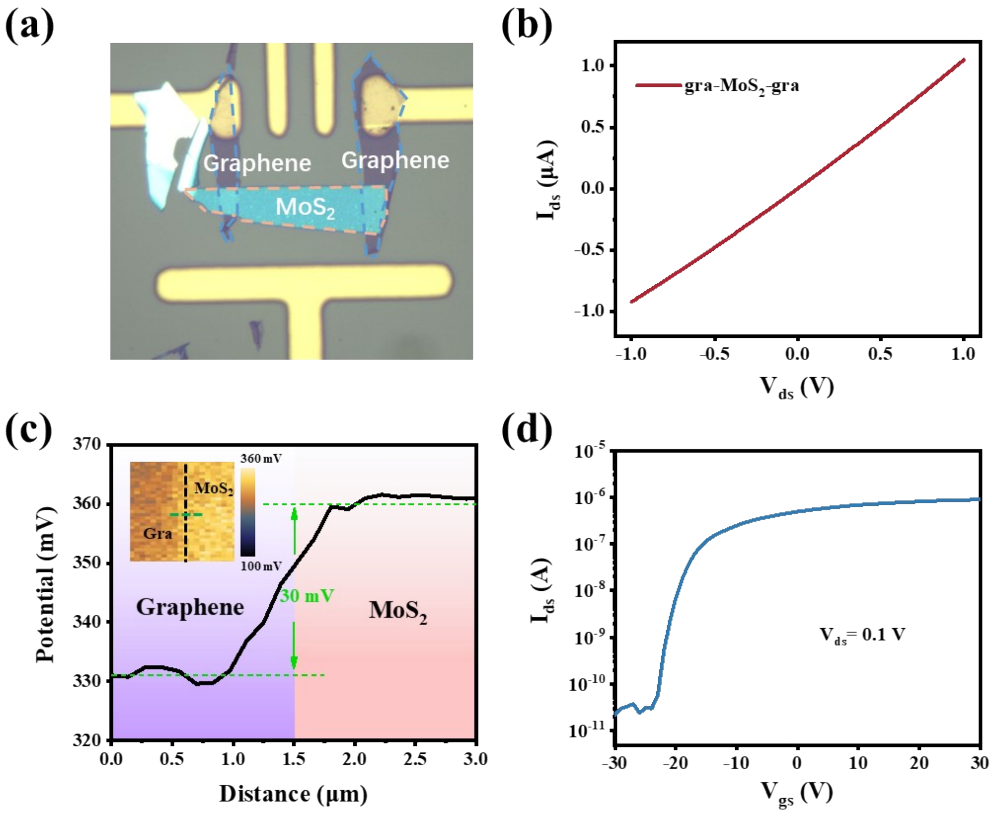

Figure S1 Characterization of graphene/MoS_2/graphene photoconductive device. (a) Optical image of the graphene/MoS_2/graphene photoconductive device. (b) I-V characteristics of the device. (c) Potential distribution between graphene and MoS_2. The inset is KPFM image of the graphene/$MoSe_2$ heterojunction. (d) Transfer characteristics of the device.

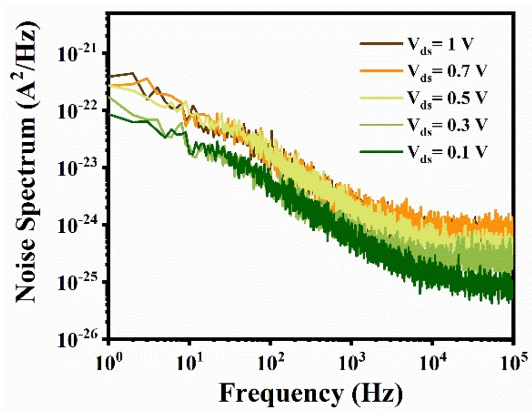

Figure S2 Noise power density-dependent frequency of the graphene/MoS_2/graphene photoconductive device at varying V_{ds} values.

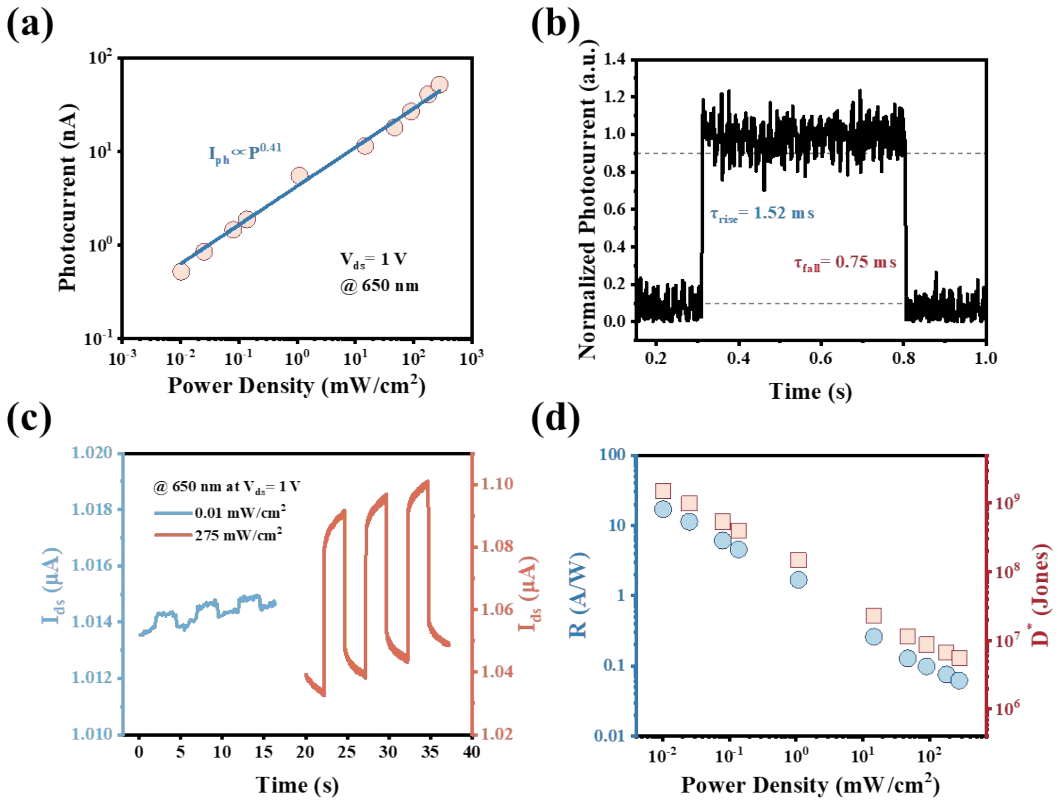

Figure S3 Photodetection characteristics of the graphene/MoS_2/graphene photoconductive detector under 650 nm illumination. (a) Photocurrent dependence on light power density. (b) Response and recovery times of the device. (c) Time-dependent photoresponse of the device under varying light power densities at V_{ds}=1 V. (d) R and D^* as functions of light power density.

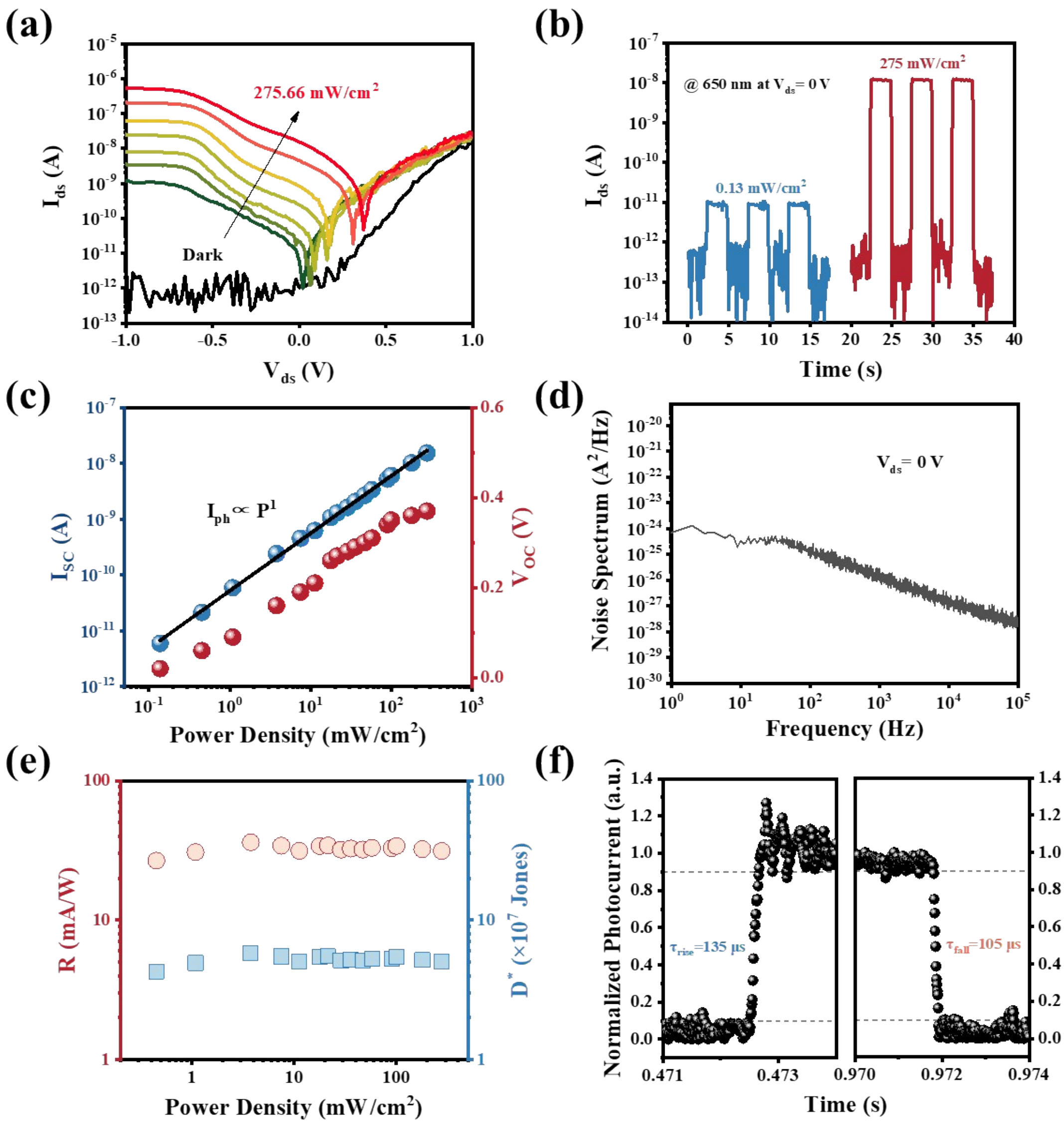

Figure S4 Photodetection characteristics of the graphene/MoS_2/$NbSe_2$ photovoltaic detector under 650 nm illumination. (a) Output characteristics of the photovoltaic detector under dark and different light power densities. (b) Time-dependent photoresponse of the device under varying light power densities at V_{ds}=0 V. (c) Dependence of short-circuit current and open-circuit voltage on light power density. (d) Noise power density-dependent frequency of the device under V_{ds}=0 V. (e) R and D^* under varying light power densities. (f) Response and recovery times of the device.

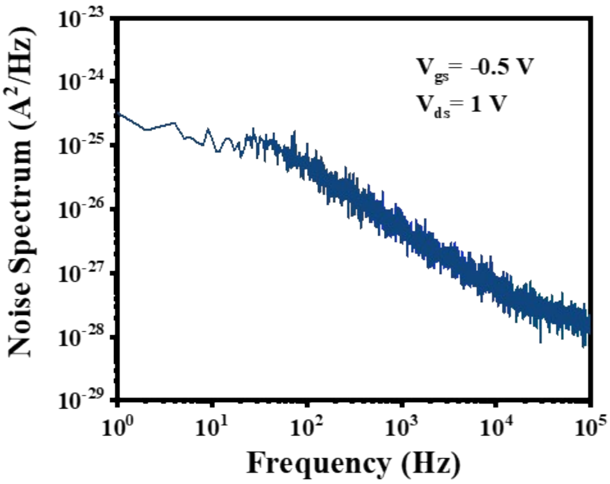

Figure S5 Noise power density-dependent frequency of the photo-MESFET at V_{ds} = 1 V and V_{gs}=-0.5 V.

1. External Quantum Efficiency

The EQE is a critical metric for evaluating the device's ability to convert incident photons into effective carriers. It is calculated using:

$$EQE = \frac{Rh\nu}{e} \times 100\% \tag{1}$$

Where R is the responsivity, hν is the photon energy (h: Planck's constant, ν: photon frequency), and e is the elementary charge. The calculated EQE reaches 1826% under 650 nm illumination, demonstrating ultra-efficient photon-to-electron conversion.

2. Photoconductive Gain

The photoconductive gain (G) of the photo-MESFET is calculated using:[1-3]

$$G = \frac{V_{ph} \times g_m \times h\nu}{e \times P} \tag{2}$$

Where V_{ph} is the photovoltage generated at the heterojunction interface, g_m is the transconductance (reflecting gate voltage modulation of channel current), and P is the incident optical power. The calculated gain is G≈47. This high gain originates from the photovoltage-driven depletion modulation mechanism—the photovoltage compresses the depletion region width, significantly enhancing channel conductivity."

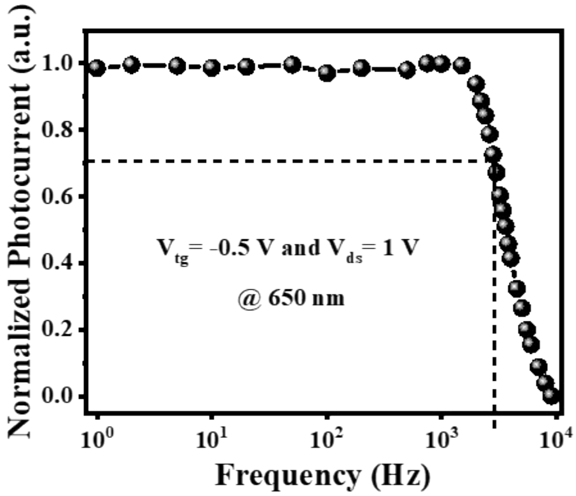

Figure S6 Normalized photocurrent as a function of the modulated frequency under 650 nm light at V_{ds} = 1 V and V_{gs}=-0.5 V.

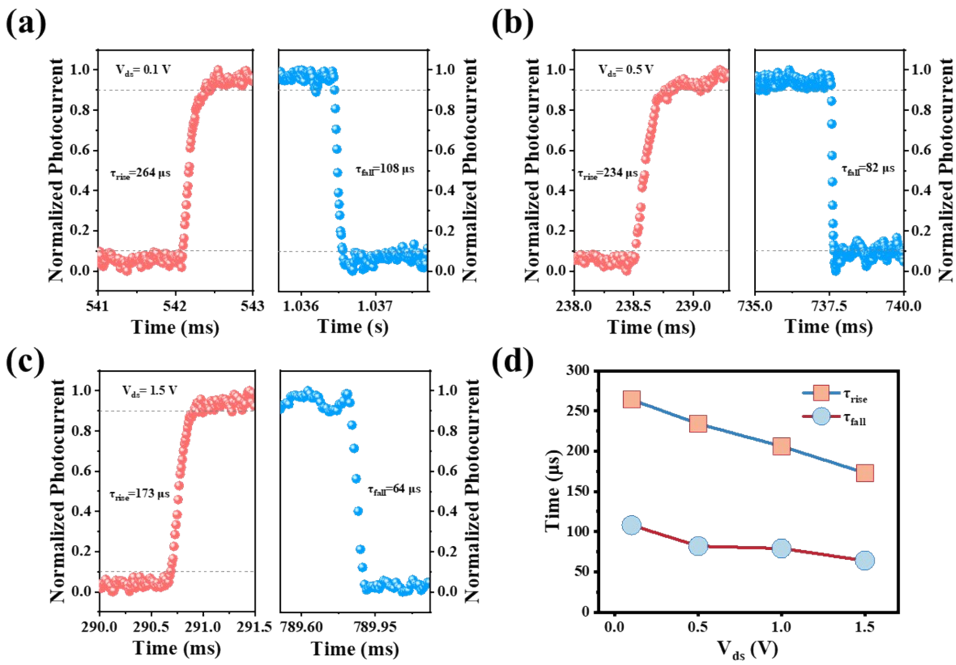

Figure S7 Response and recovery times of the photo-MESFET under varying drain-source bias: (a) V_{ds}=0.1 V, (b) V_{ds}=0.5 V, and (c) V_{ds}=1.5 V. (d) V_{ds}-dependent trends of τ_{rise} and τ_{fall}.

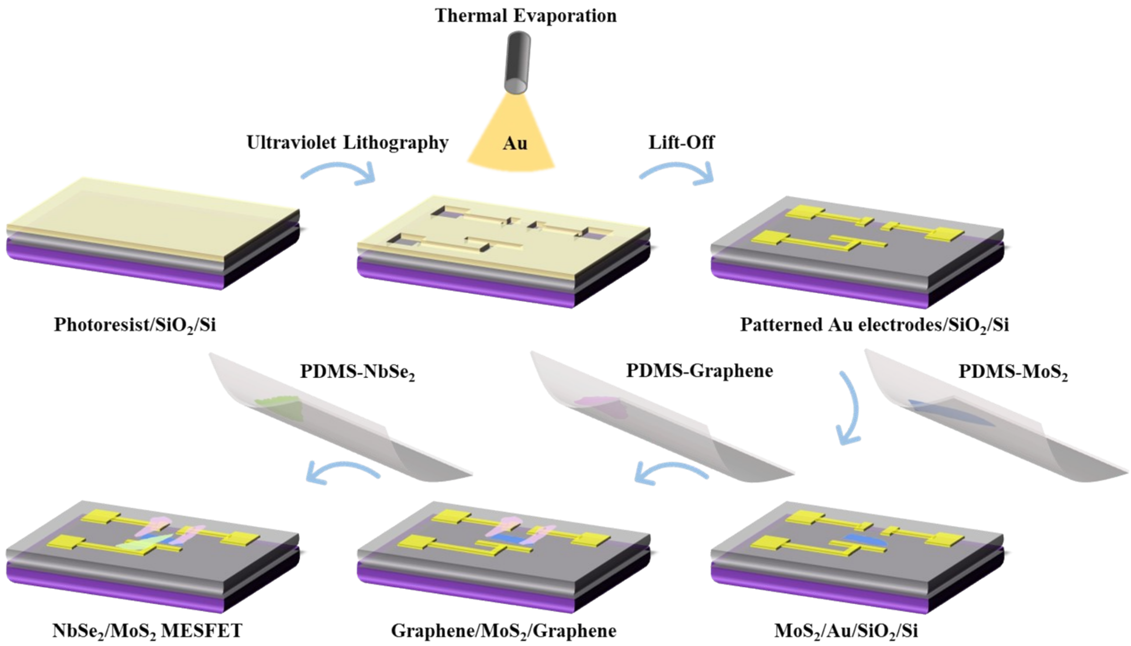

Figure S8. Schematic diagram of the fabrication process of the all-2D vdWs MESFET device.

Table S1 Comparisons of important performance parameters of the proposed photo-MESFET with other reported photodetectors

Structure	I_{on}/I_{off}	R (A/W)	D^* (Jones)	τ_{rise}/τ_{fall}	References
$NbSe_2/MoS_2$ MESFET	4.1×10^5	9.56@650 nm	2.23×10^{10}	206/79 μs	This work
NiO_x/MoS_2 MESFET	2.85×10^3	1.1@520 nm		2 ms	4
Graphene/Si sMESFET	~11	~10^3@532 nm	2.3×10^{12}	6/232 μs	3
Ge/MoS_2 JFET		66@532 nm	5.3×10^9	40/160 μs	5
$PdSe_2/MoS_2$ JFET	10^2	600@532 nm	10^{11}	100/37 ms	6
MoS_2 Photoconductor	6×10^3	10^3@647 nm		13/11 s	7
$TaIrTe_4/MoS_2$ Photodiode	10^4	0.75@635 nm	7×10^{11}	7.9/7.1 ms	8

References

1. V. Adinolfi and E. H. Sargent, *Nature*, 2017, **542**, 324-327.
2. N. Guo, L. Xiao, F. Gong, M. Luo, F. Wang, Y. Jia, H. Chang, J. Liu, Q. Li, Y. Wu, Y. Wang, C. Shan, Y. Xu, P. Zhou and W. Hu, *Adv. Sci.*, 2020, **7**, 1901637.
3. J. Fu, C. Nie, F. Sun, H. Jiang, Y. Li, G. Li and X. Wei, *Adv. Opt. Mater.*, 2023, **11**, 2201983.
4. H. S. Lee, S. S. Baik, K. Lee, S. W. Min, P. J. Jeon, J. S. Kim, K. Choi, H. J. Choi, J. H. Kim and S. Im, *ACS nano*, 2015, **9**, 8312-8320.
5. B. Wang, L. Wang, Y. Zhang, M. Yang, D. Lin, N. Zhang, Z. Jiang, M. Liu, Z. Zhu and H. Hu, *Adv. Funct. Mater.*, 2021, **32**, 2110181.
6. H. Wang, Z. Li, D. Li, X. Xu, P. Chen, L. Pi, X. Zhou and T. Zhai, *Adv. Funct. Mater.*, 2021, **31**,

2106105.
7. J. F. G. Marin, D. Unuchek, K. Watanabe, T. Taniguchi and A. Kis, *npj 2D Mater. Appl.*, 2019, **3**, 14.
8. L. Zhang, X. Han, S. Zhang, H. Wang, Y. Huang, Z. Zheng, N. Huo, W. Gao and J. Li, *Adv. Electron. Mater.*, 2022, **8**, 2200551.